

# THERMO-MECHANICAL ASPECTS OF THE MOBIPIX, A COMPACT X-RAY IMAGING SYSTEM WITH EMBEDDED GPU\*

A. Gilmour A Jr.<sup>†</sup>, W.R. Araujo, J.M. Polli,  
 Brazilian Synchrotron Light Source (LNLS), Campinas, Brazil

## Abstract

In the light of the high brilliance fourth generation synchrotron light sources, real-time imaging techniques became possible, boosting the demand for fast and reliable detectors. Mobipix project is a compact X-ray imaging camera designed for Sirius [1], based on Medipix3RX\*\* [2,3]. The control and acquisition system uses System-On-a-Chip technology with embedded Graphics Processing Units (GPUs) where data processing algorithms will run in real time. The Mobipix X-ray detector is designed to perform as a video camera, enabling X-ray imaging experiments and beam diagnose, at thousands of frames per second (FPS), without external computers.

This paper presents the development of the Mobipix detector mechanics. The authors describe the path taken to design the structural aspects, ensuring robustness and versatility in the device installation to the beamlines, and the thermal aspects, regarding forced air cooling, high heat density, and small volume through which the flow will occur. The latter aspects were developed by exploiting Computational Fluid Dynamics (CFD) modelling.

The Mobipix has 28 x 28 mm<sup>2</sup> active area, composed by 260k pixels of 55 x 55 μm<sup>2</sup>, and is planned to achieve continuous readout up to 2000 FPS.

## INTRODUCTION

The Mobipix electronic design is composed of three boards, the upper board is the carrier board, responsible for housing a Nvidia Jetson TX-1 [4] and providing external connections. The lower board contains the analogical and digital electronics for Mobipix control and readout, being nominated Mobipix board. The board housing four Medipix3RX sensors is attached to the Mobipix board by a perpendicular connection, and is called the Medipix board. Figure 1, illustrates the three boards and their assembly disposition.

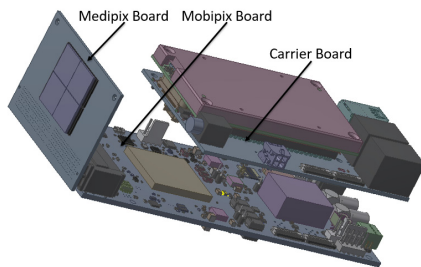


Figure 1: The three electronic boards that compose Mobipix, assembled.

\* Work supported by Brazilian Ministry of Science, Technology, Innovations and Communications.

\*\*LNLS is a member of CERN Medipix3 Collaboration.

<sup>†</sup> allan.gilmour@lnls.br

## Simulation

### Thermal

## Objectives

This work aimed at keeping the volume of the device as small as possible, while ensuring that the temperature of each component is kept within its given limits. There are two different kinds of semiconductor sensors intended to be coupled to Mobipix, one made of silicon (Si) and another made of cadmium telluride (CdTe). The thermal project must attend both possibilities.

Figure 2 and Figure 3 demonstrate the position of the main heat generating components, while Figure 4 lists their description and worst-case scenario heat dissipation, according to their datasheets [2-13].

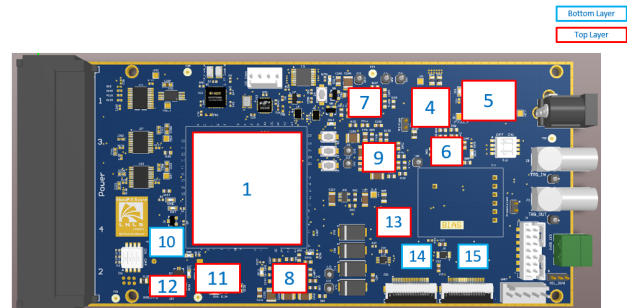


Figure 2: Heat generating components in Mobipix board.

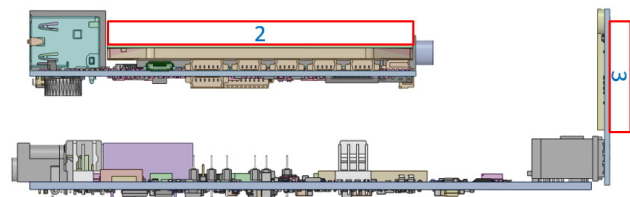


Figure 3: Heat generating components in the other two boards.

Component (ID no.)	Power [W]	P. Density [W/m <sup>3</sup> ]	Allowed T [°C]
FPGA Kintek-7 Xilinx (1)	4	1.32E+06	80
Jetson TX-1 (2)	15	4.27E+05	80
Sensor Medipix-3RX (3)	6	6.56E+06	60
LTC4358 Protection Diode (4)	1	1.83E+07	80
BNX025H01B Source Filter (5)	1	2.65E+06	80
LTM4622 Tension Adjuster (6)	1.8	1.90E+07	120
LTM4622 Tension Adjuster (7)	0.9	9.52E+06	120
LTM4622 Tension Adjuster (8)	1.2	1.27E+07	120
LTM4622 Tension Adjuster (9)	1.5	1.59E+07	120
ADP1740ACPZ-1.5 Tension Adjuster (10)	0.2	1.48E+07	80
LT3071 Tension Adjuster (11)	0.82	5.69E+07	80
ADP1740ACPZ-2.5 Tension Adjuster (12)	0.16	1.19E+07	80
LT3080 Tension Adjuster (13)	1.1	1.43E+08	125
MC20902 MIPI Protocol Driver (14)	0.5	1.36E+07	80
MC20902 MIPI Protocol Driver (15)	0.5	1.36E+07	80

Figure 4: Heat Generation, Heat Density and Maximum Allowed Temperature for Each Component.

Content from this work may be used under the terms of the CC BY 3.0 licence (© 2018). Any distribution of this work must maintain attribution to the author(s), title of the work, publisher, and DOI.

### Inner Assembly

As one of the main objectives is the achievement of a portable size, it was decided that the chassis, upon which the boards will be assembled, will also act as a heat spreader, dissipating the power generated by the electronics.

The sensor heat exchanger is a copper piece fitted through two holes in the backside of the Medipix board, touching the ASICs as a cold finger. On its backside, the airflow removes the heat, through fins.

Figure 5 presents the intended interior assembly, in which the sensor heat exchanger is displaced to allow the visualization of the fitting.

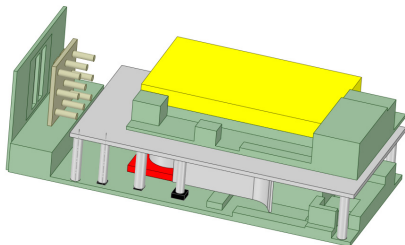


Figure 5: Projected interior assembly, with the heat exchangers.

As the front face is reserved for the sensor, and the back panel will be populated with connectors, both these sides cannot house cooler fans, and the boards arrangement, one above the other, also makes it ineffective to use the upper and bottom faces as primary dissipation sides.

The superior limit of velocity commonly adopted for air cooling of electronic components is 3 m/s. Higher values will generate interference (noise) and vibration. The convective coefficient in this case is approximately 15 W/m<sup>2</sup>K [14].

## METHODOLOGY

The software Space Claim Design Modeler was utilized to prepare the model for simulation and make adjustments, and the software Ansys Fluent was used to perform the Computational Fluid Dynamics simulations.

Series of simulations were performed to determine the number of cooler fans needed, their dimensions and their locations, as well as the chassis height. Then, another series of simulations were performed to define the position, shape and size of the heat exchanger touching pads. Lastly, new series of simulations were performed to test possible enhancements, such as application and dimensioning of guiding vanes and fins, and the use of alternative materials to benefit the heat exchange with each component.

The streamlines and vectors obtained through CFD were used to understand the flow inside the system. This helped to identify zones of recirculation, stagnation and interference. With this data, it was possible to move and take advantage of the mentioned zones to reach more efficient results. The shapes of the chassis-heat spreader and the sensor heat spreader were entirely based on this analysis.

## RESULTS

The simulations determined the cooler fans position presented in Figure 6, with optimal results occurring when they faced each another, and that two 50x50x12 mm coolers, blowing 13 cubic feet per minute (CFM) each, at ambient temperature 24±0.1°C, would suffice for the system cooling, with expected temperatures presented in Table 1, for both kinds of sensors, silicon and cadmium telluride.

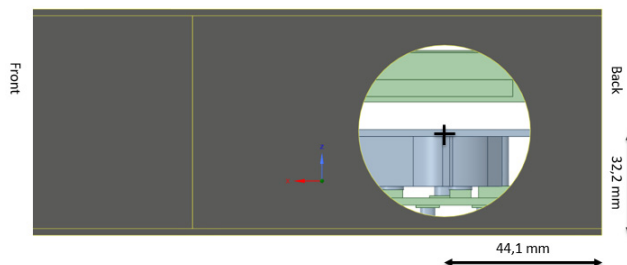


Figure 6: Positions of inlets that generated better results.

Table 1: Expected Temperatures for 13 CFM (3 m/s)

Component	Temperature [°C]
1	33.9
2	59.5
3	55.3(Si)/56.6(CdTe)
4	58.6
5	51.7
6	66.4
7	54.6
8	68.3
9	60.5
10	44.9
11	48.3
12	35.2
13	84.7
14	57.5
15	60.6

It can be noted that every component is well within their temperature limits, except for the sensor. Future works may include improvements to the sensor heat exchanger, which would allow the same results or better with slower inlet speeds.

Different materials such as copper alloys were also tested for the composition of the main chassis-heat spreader, however, the difference in the components temperature (in average, 0.5°C) did not justify the increase in weight (approximately three times heavier) and manufacture difficulty. Also, it was observed that the convection with the exterior walls represents a negligible effect on the inside temperatures. Nonetheless, this heat exchange was kept in the simulations.

As can be observed in Figure 7, the temperature at the larger components, such as Jetson and FPGA was well below the rest of the components in the system, due to the larger area presented to the flow. With this information it is possible to avoid the use of extra fins.

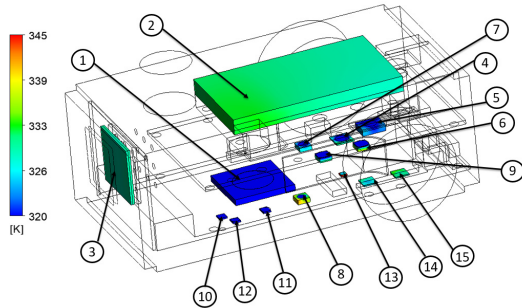


Figure 7: Heat Distribution Comparison inside the system.

Figure 8 and Figure 9 present the air flow inside the device. The cylindrical cold fingers of the chassis-heat spreader were positioned in a way that preserves the main air path toward the next components, using the recirculation to direct the flow towards other components, increasing the heat exchange efficiency.

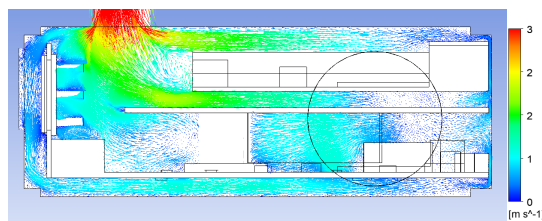


Figure 8: Velocity Vectors in the Longitudinal Plane.

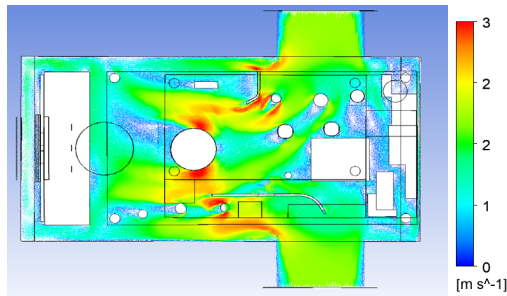


Figure 9: Velocity Vectors in the Transversal Plane.

Inside the system, as depicted in the same Figure 8 and Figure 9, the observed velocity of the stream is above the limit of 3 m/s. However, as observed in Figure 10, the velocity next to the board and components is below the limit.

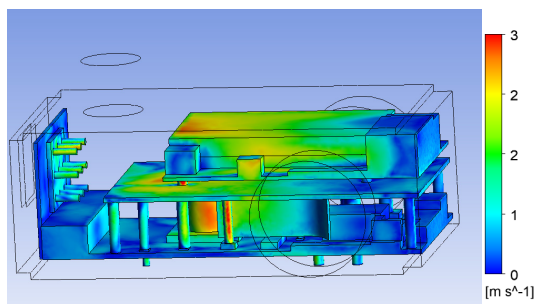


Figure 10: Velocity next to the components.

## CONCLUSION

The results obtained in the simulation were satisfactory and, thus, a first prototype was built and awaits the electronic boards assembly for tests and model validation. Meanwhile, a second version of sensor heat exchanger is under development.

The external structure that allows an easy assembly and robust fixture to the beamline, preventing the obstruction of the air vents was also developed, and a preview image is presented in Figure 11.

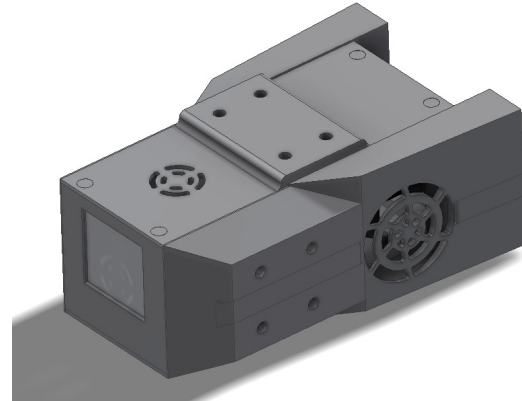


Figure 11 : Mobipix Structure.

## ACKNOWLEDGEMENTS

The authors would like to thank all the colleagues that helped with the acquisition of data and experience in the developing of synchrotron devices and also those who helped revising this paper and the poster. Also thanks for the good moments and friendship.

Special thanks to Luciano Camacho, Débora Magalhães, Marcos Errada, Marlon Saveri, Alexis Sikorski and Francisco Figueiredo.

## REFERENCES

- [1] L. Liu, *et al.*, “The Sirius project.”, in *J. Synchrotron Radiation*, vol. 21, no.5, pp. 904–11, 2014.
- [2] R. Ballabriga, *et al.*, “The Medipix3RX: a high resolution, zero dead-time pixel detector readout chip allowing spectroscopic imaging”, *Journal of Instrumentation*, vol. 8, 2013, doi:10.1088/1748-0221/8/02/C02016
- [3] CERN Medipix3 Collaboration, <https://medipix.web.cern.ch/collaboration/medipix3-collaboration>
- [4] Nvidia, “Jetson-TX1 Thermal Design Guide”, <http://developer.nvidia.com>
- [5] Xilinx, “Power Estimator FPGA-7 Series”, <http://www.xilinx.com>
- [6] Analog Devices, “LTC4358 Protection Diode Datasheet”, <http://www.analog.com>
- [7] Murata, “BNX025H01B Source Filter Datasheet”, <http://www.murata.com>
- [8] Analog Devices, “LTM4622 Tension Adjuster Datasheet”, <http://www.analog.com>
- [9] Analog Devices, “ADP1740ACPZ-1.5 Tension Adjuster Datasheet”, <http://www.analog.com>
- [10] Analog Devices, “LT3071 Tension Adjuster Datasheet”, <http://www.analog.com>
- [11] Analog Devices, “ADP1740ACPZ-2.5 Tension Adjuster Datasheet”, <http://www.analog.com>

Content from this work may be used under the terms of the CC BY 3.0 licence (© 2018). Any distribution of this work must maintain attribution to the author(s), title of the work, publisher, and DOI.

- [12] Analog Devices, “LT3080 Tension Adjuster Datasheet”,  
<http://www.analog.com>
- [13] Meticom, “MC20902 MIPI Protocol Driver Datasheet”,  
<http://www.meticom.com>

- [14] J. Parry, R. Bornoff, B. Blackmore, “Move your Thermal Strategy for Air-Cooled Electronics up in the Design Flow”,  
*Electronic Design*, vol. 57, no. 14, p. 39, Jul. 2009.